Recent Advances in Catalyst Materials for PEM Water Electrolysis

Paula Marielle Ababao and Ilwhan Oh*

Department of Applied Chemistry (Department of Energy Convergence Engineering)
Kumoh National Institute of Technology, Gumi, Gyeongbuk, South Korea

ABSTRACT : Due to the intermittency of renewable energy sources, a need to store and transport energy will increase. Hydrogen production through water electrolysis will provide an excellent way to supplement the intermittency of renewable energy sources. While alkaline water electrolysis is currently the most mature technology, it has drawbacks of low current density, large footprint, gas crossover, etc. The PEM water electrolysis has potential to replace the alkaline electrolysis. However, expensive catalyst material used in the PEM electrolysis has been the bottleneck of widespread use. In this review, we have reviewed recent efforts to reduce catalyst loading in PEM water electrolysis. In core-shell nanostructures, the precious metal catalyst forms a shell while heteroatoms form a core. In this way, the catalyst loading can be significantly reduced while maintaining the catalytic activity. In another approach, a corrosion-resistant support is utilized, which provides a stable platform to impregnate precious metal catalyst.

Keywords : Hydrogen Economy, Water Electrolysis, Renewable Energy, Catalyst, Oxygen Evolution Reaction

1. Introduction

1.1 Transition to hydrogen economy

The term "hydrogen economy" means an eco-friendly socio-economic system that uses hydrogen as an energy carrier in contrast with existing fossil fuel-based energy systems. Global hydrogen use has been steadily increasing, and has increased about three times since 1975 (currently $110 billion market).[1] Since hydrogen does not exist naturally, it must be produced from existing energy sources. Currently, the most widely used hydrogen production method is steam methane reforming (Grey hydrogen), which is the most economical, but there is a problem of emitting carbon (unit price ~$2/kg H_2). So, a combination of reforming and carbon capture (CCUS) is emerging as a mid-term alternative (Blue hydrogen).

Hydrogen production through water electrolysis with renewable energy power will be an eco-friendly hydrogen production method without carbon

*E-mail: ioh@kumoh.ac.kr

Table 1. Classification of hydrogen according to production methods

Classification	Production method	Merit/Demerit
Grey hydrogen	Steam methane reforming	Low price, economics of scale Carbon emission
Blue Hydrogen	Steam methane reforming + CCUS	Interim technology
Green Hydrogen	Water electrolysis (using renewable energy)	Zero carbon emission High price

emissions (Green hydrogen). While the price of renewable energy continues to decline worldwide, the high price of water electrolysis systems remains a problem.[2] It is largely divided into three categories by the existing water electrolysis method. Alkaline electrolysis has already been commercialized and is used in hydrogen production. Since the Ni-based non-precious metal catalyst is used, it is inexpensive, and the life of the cell stacks in the alkaline electrolysis is long. The disadvantages are that the space occupied by the electrolyzer stack is
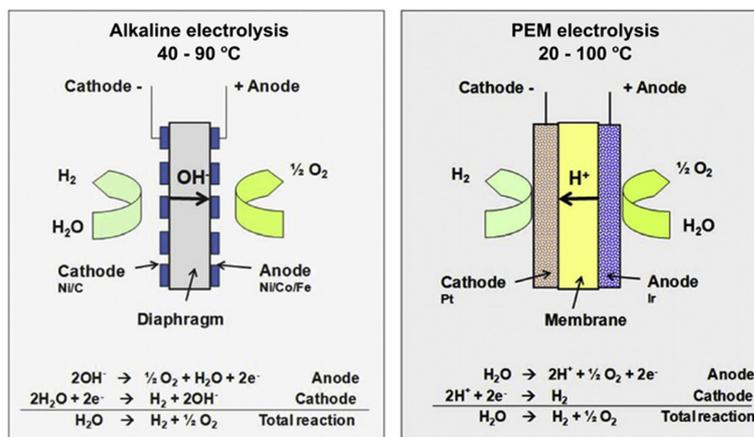
**Fig. 1. Working principles of alkaline electrolysis (left) and PEM electrolysis (right). Reproduced with permission.[2)]
Copyright 2013, International Journal of Hydrogen Energy.**

Table 2. Merits and demerits of alkaline and PEM electroyzers

	Alkaline electrolysis	PEM electrolysis
Merits	· Mature technology · Cheap catalyst · Long-term stability · Low cost	· High current density (compact system) · Low gas crossover (high gas purity) · Good partial load range
Demerits	· Low current density · Gas crossover · Limited partial load range · Low operational pressure	· High cost of components · Corrosive media · Low lifetime

large, the purity of hydrogen produced is degraded due to gas crossover, and low- current operation is challenging due to the generation of hydrogen/oxygen mixed gas. In green hydrogen production, load flexibility of water electrolyzer is important due to the intermittency of renewable energy. Anion-exchange membrane (AEM) water electrolysis, a next-generation water electrolysis method, can be seen as a device that combines the advantages of the alkaline electrolysis and the PEM electrolysis. There is an advantage in that a low-cost non-precious metal catalyst may be used in an alkaline environment while gas crossover may be minimized by using a polymer film transferring hydroxide ions (OH^-). It is still in the early stages of technology development, and there is much room for performance and unit price improvement.

PEM water electrolysis is a method of operating in an acidic media by utilizing proton-conducting membranes such as Nafion. Since the current density is larger than that of alkaline water electrolysis, the device size becomes smaller, the purity of hydrogen produced is high due to low gas crossover, and it is compatible with intermittent power of renewable energy. The disadvantage is that the device is quite expensive due to expensive precious metal catalysts and titanium current collectors that can withstand corrosion due to strong acid/high voltage operating environments.

1.2 PEM water electrolysis

PEM water electrolysis was developed by General Electric, Inc. in the 1960s to compensate for the shortcomings of the existing alkaline electrolysis.[3,4)] PEM water electrolyzers utilized a solid polymer electrolyte, which enables high proton conductivity, low gas crossover, and high-pressure operation.

Compared to alkaline electrolyzers, PEM electrolyzers can operate at much higher current densities (~2 A/cm^2). Therefore, the cell area decreases and the system becomes compact. In addition, PEM electrolyzers are suitable for partial load operation because there is less gas crossover passing through the polymer electrolyte membrane. In alkaline electrolysis, the purity of the produced hydrogen can

be lowered because the amount of hydrogen generated in the low current operation is reduced while the gas crossover remains unchanged. Furthermore, there is a risk of explosion due to the generation of mixed gas. As a result, PEM electrolyzer is compatible with renewable energy with high variability in power output. (nominal power density range 10~100%)

PEM electrolyzer's solid polymer membrane has strong chemical/mechanical properties, which enables high operation pressure of up to 350 bar for some commercial models.[5,6] High pressure operation enables high-pressure hydrogen gas production, which saves energy for further compression storage of hydrogen gas.

On the other hand, the proton-exchange membrane used in the PEM electrolyzer creates a corrosive strong acid atmosphere (pH~2), and the operating voltage is also high (~2 V), so the material that can be used in the PEM electrolyzer is very limited. Only noble metals such as Ir, Ru, and Pt can be used for the catalyst layer, and only Ti material can be used for the current collector. In particular, Ir is one of the rarest elements on Earth's surface which is 1/10 times the deposit of platinum. If PEM electrolyzer is rapidly distributed to the market in the future, it is expected to have a significant impact on iridium supply and price.[7-9]

1.3 Mechanism of OER

Oxygen evolution reaction (OER) is one of the half-reactions of water splitting and is regarded as the bottleneck due to its sluggish kinetics resulting from the complexity of the four-electron process. The reactions at the cathode and anode for the water-splitting reaction differ under acidic and alkaline environments. Numerous research groups have hypothesized potential processes for oxygen evolution reaction at the anode electrode under acid or alkaline conditions, and there are both differences and similarities between these proposed mechanisms. Most of the proposed mechanisms include the same intermediates, such as MOH and MO, although there is likely a significant variance in the process that produces oxygen. It is observed that there are two distinct ways to produce oxygen from a MO intermediate (Fig. 2). One includes the direct combination of 2MO to produce $O_2(g)$, and the
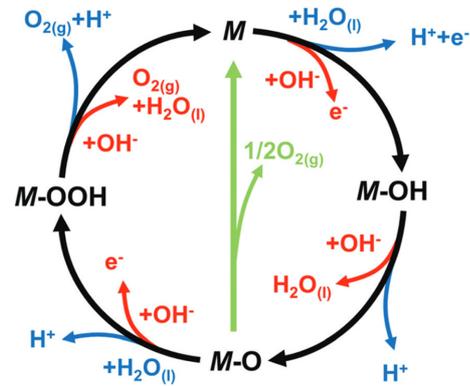

Fig. 2. OER mechanism for alkaline (red line) and acidic (blue line) environments. The green line shows a different pathway for the direct reaction of two nearby oxo (M-O) intermediates to produce oxygen, whereas the black line shows that oxygen evolution involves the synthesis of a peroxide (M-OOH) intermediate. Reproduced with permission.[75] Copyright 2017, Royal Society of Chemistry.

other involves the production of the MOOH intermediate, which decomposes to $O_2(g)$. Despite this disagreement, there is widespread agreement that the electrocatalysis of OER is a heterogeneous reaction in which the bonding interactions (M–O) within the intermediates (MOH, MO, and MOOH) are critical for the overall electrocatalytic activity.[10,11]

Step 1: Water will produce OH* active species on the surface of an electrode.
Acidic conditions:
$$H_2O + M \rightarrow M - OH^* + H^+ + e^- \tag{1}$$
Alkaline conditions:
$$OH^- + M^+ \rightarrow M - OH^* + e^- \tag{2}$$
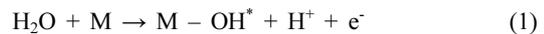
Step 2: OH* on the electrode surface will convert to O*
Acidic conditions:
$$M - OH^* \rightarrow M - O^* + H^+ + e^- \tag{3}$$
Alkaline conditions:
$$M - OH^* + OH^- \rightarrow M - O^* + H_2O + e^- \tag{4}$$
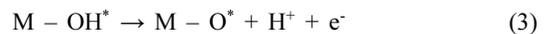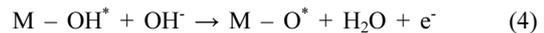
Step 3: The absorbed O* will react with H_2O or OH^- and convert to OOH*
Acidic conditions:
$$M - O^* + H_2O \rightarrow M - OOH^* + H^+ + e^- \tag{5}$$
Alkaline conditions:
$$M - O^* + OH^- \rightarrow M - OOH^* + e^- \tag{6}$$
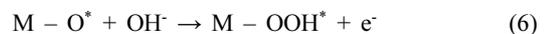
Step 4: O_2 is produced after OOH^* desorption

Acidic conditions:
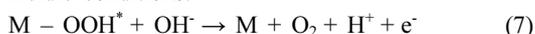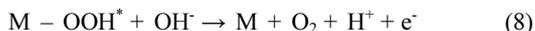
$$M - OOH^* + OH^- \rightarrow M + O_2 + H^+ + e^- \qquad (7)$$

Alkaline conditions:

$$M - OOH^* + OH^- \rightarrow M + O_2 + H^+ + e^- \qquad (8)$$

Fig. 2. OER mechanism for alkaline (red line) and acidic (blue line) environments. The green line shows a different pathway for the direct reaction of two nearby oxo (M-O) intermediates to produce oxygen, whereas the black line shows that oxygen evolution involves the synthesis of a peroxide (M-OOH) intermediate. Reproduced with permission.[75] Copyright 2017, Royal Society of Chemistry.

1.4 Electrocatalysts for PEM water electrolysis

In the initial PEM electrolysis, noble metals such as Ir and Pt were mainly used as catalysts and they accounted for a large part of the entire system cost. Therefore, from the beginning of development, efforts have been made to reduce the loading of these noble metal catalyst materials or to replace them with cheaper materials. Furthermore, a half-cell test method with liquid electrolyte has been developed, which enabled the simple and fast screening of catalyst candidates in a liquid electrolyte.[12] Various single elements were evaluated for catalyst materials, and it has been reported that Ir, Ru, Pt are the most efficient for OER and Ir, Pt are the most efficient for hydrogen evolution reaction (HER).

For OER catalysts, the properties of noble metal 'oxide' have a great influence on electrocatalytic activity.[12] That is, Ir or Ru represents an overpotential lower than Pt. For Pt, the catalytic activity is lower due to the low conductivity of the surface oxide, while Ru and Ir show high activity by forming surface oxide with high conductivity as high as ~104 S/cm for single crystals.[13] In the oxide of Ru and Ir, the d-orbital overlap of metal atoms is possible, leading to the d-electron conduction. The problem with RuO_2 is that it gradually corrodes and leaches out as the OER reaction progresses. There have been studies on adding additional oxides to mitigate the corrosion of RuO_2, and some progress have been made.[13] Ru, Ir, and their oxides were investigated for their electrochemical properties
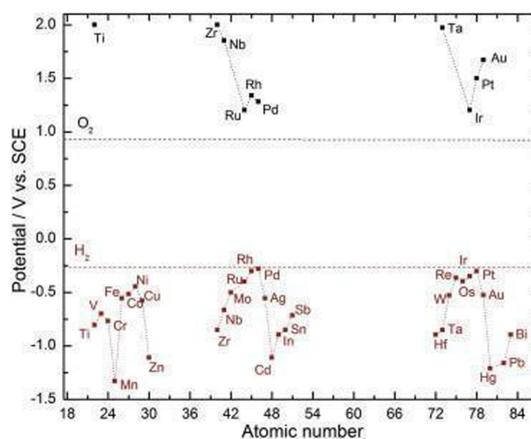
Fig. 3. Evaluation of various single-element catalysts for HER and OER. Reproduced with permission.[12] Copyright 1976, The Electrochemical Society.
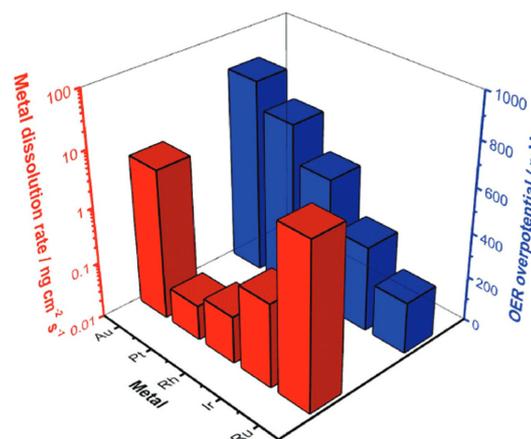
Fig. 4. OER performance in form of overpotential and metal dissolution rates. Reproduced with permission.[16] Copyright 2016, John Wiley & Sons, Ltd.

which exhibit a stability increase in the following order: Ru < RuO_2 < Ir < IrO_2.[14] RuO_2 and IrO_2 report high metallic conductivity in the order of ~104 $W^{-1}cm^{-1}$ with RuO_2 demonstrating the lowest oxygen overpotential than any other materials. When compared to other noble metals, Figure 4 shows the following trend for stability under OER conditions: Pt > Rh > Ir > Au > Ru where Ru offers the lowest overpotential at the same time the highest dissolution rate.[15] However, since the corrosion problem of RuO_2 has not been completely solved, in most cases, the Ir catalyst has been used
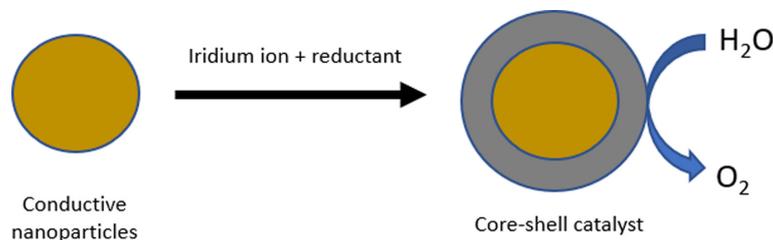
Fig. 5. Synthesis of Ir core-shell catalyst to reduce the catalyst loading.

for the anode and the Pt catalyst has been used for the cathode in practical PEM electrolyzers. It was shown that the cathode catalyst loading can be significantly lowered, and the loading is currently about 0.5 to 1.0 mg/cm^2. On the anode side, Ir catalyst is still mainly used, but loading has not been lowered much since the early development due to large overpotential, and loading is currently at the level of 2 mg/cm^2.

In the PEM electrolyzer, most of the overpotential is applied to the anode and the OER reaction still exhibits high overpotential and slow kinetics. Therefore, it is difficult to lower the catalyst loading further. In addition, it is difficult to find a catalyst material that can replace Ir because most elements in the periodic table cannot withstand the strong acid environment at high voltage at which the PEM electrolyzer operates. Therefore, in order to lower the price of anode materials, which account for a significant portion of the current PEM electrolyzer cost, the core-shell structure of iridium and second material is suggested as an alternative. In this core-shell nanostructure, core materials do not participate in the OER reaction but provide a stable support. In addition, these core materials must have decent electron conductivity, and candidate materials include noble metals (Ru, Pt, Au, Ni, Ag, etc), metal oxide (TiO$_2$, SnO$_2$, ZnO, ITO, etc). As Ir is placed on the shell, its loading is expected to be significantly reduced compared to pure Ir catalyst material. In this context, this review summarizes previous studies that utilize the core-shell nanostructure catalyst for PEM electrolysis.

1.5 Hints from corrosion-resistant catalyst supports developed for fuel cells (non-carbon)

As a promising portable power source for elec-

trochemical energy conversion, polymer electrolyte membrane fuel cells (PEMFCs) have been a research focus in the scientific and industrial communities since the 1960s. Carbon-supported materials are the most widely used catalyst in PEMFC due to its high electrical conductivity, accessibility, and affordability.[17] However, carbon-supported materials are limited by their poor stability causing severe carbon corrosion over the course of normal PEMFC operations which is formulated as:

$$C + 2H_2O \rightarrow CO_2 + 4H^+ + 4e^-, E^0$$
$$= 0.207 \text{ V vs. SHE} \tag{9}$$
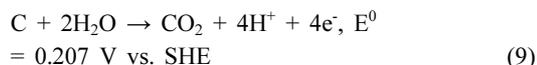
Thus, it is a challenge to find an appropriate substitute for traditional carbon support which should possess the following properties: high electrical conductivity and stability, strong electronic catalyst–support interaction, and suitable economic criteria.[18] In this regard, metal oxides, carbides, and nitrides have been explored as an alternative for carbon supports.

Considering that metal oxides have less superior conductivity than carbon, support conductivity greater than that of the fuel cell membrane is a key requirement due to the limitations of the fuel cell membrane resistance (0.1 S/cm). Since most metal oxide supports have lower surface area than carbon materials, synthesizing mesoporous metal oxides can present a relatively higher surface area which enhances the catalytic activity for ORR due to its strong metal–support interaction (SMSI).[19]

Metal oxide. Replacements for carbon as fuel cell support have extensively investigated metal oxides such as SnO$_2$, WO$_2$, TiO$_2$, SiO$_2$, and MoO2.[20-25] Compared to all metal oxides tested, TiO$_2$ attracted more attention for its high chemical and electrochemical stability, strong interaction with

metal nanoparticles, nontoxicity, availability, and cost-effectiveness. Electronic conductivity in TiO_2 has proven to significantly increase after doping with transition metals such as Zr[25], Hf[26], V[27], Nb[27–35], Ta[36,37], Cr[38], Mo[24,39], W[21], and Ru[37,40]. Early studies have demonstrated the stability of these doped TiO_2 systems under PEMFC operating conditions: Nb-doped-TiO_2 (NTO), Ta-doped-TiO_2 (TTO), W-doped-TiO_2 (WTO) and Mo-doped-TiO_2 (MTO). Among these relatively high conductivity candidates, WTO (0.02 S/cm) and MTO (2.8×10^{-4} S/cm) were deemed too low for catalyst support applications. Another factor that must be considered is the density of TiO_2 which is about two folds higher than carbon. This results in a TiO_2 catalyst layer that is 8 μm thinner than one consisting of carbon leading to lower mass transfer limitations.[16,20,23]

Metal carbide. Due to its excellent conductivity and acid resistance, metal carbide is one of the potential replacements for carbon as a support for fuel cell catalysts. Liu et al. showed that a Pt nanoparticle's activity on tungsten carbide is increased when compared to a Pt/C catalyst.[1] Tungsten carbide, however, is unstable within the theoretical operating range of fuel cells. During the ORR, formed WO_x causes Pt agglomeration and detachment.[41-43] Cheng et al. used the atomic layer deposition method to deposit Pt nanoparticles on ZrC. The catalyst displayed 5-fold higher stability and 2-fold higher activity than Pt/C, and the author attributed this superior performance to the strong metal-support interaction (SMSI) between the support and Pt catalyst.[44] However, no more research has been done to demonstrate that the outstanding performance of

Pt/ZrC may be applied to fuel cells. The activity and stability of Pt supported on TiC, NbC, and SiC were also examined, however, none offered adequate Pt particle dispersion or consistent ORR performance.[44-48]

Metal nitride. TiN has been extensively studied and has demonstrated corrosion resistance in acidic environments as well as electrochemical stability across a broad operating potential range. Nan et al. produced a bi-metallic titanium nitride nanotube as stable catalyst support, demonstrating a mass activity of 0.78 A/mg Pt, which is 3.6 times greater than the commercial Pt/C, and retaining 3.2 times stronger ECSA than Pt/C after 15,000 stability cycles.[49] In addition, Xiao et al. demonstrated the existence of SMSI between a TiN-based support and Pt cluster.[50] However, Luo et al. argue that the interaction between TiN and Pt inhibits the ORR, and Yang et al. demonstrated that Pt/TiN enables the ORR to proceed via two electron transfer pathways, which will result in decreased electron efficiency.[51] In the RDE evaluation, the majority of metal nitride exhibited appropriate stability, although few of them have been evaluated under fuel cell operating conditions.

2. Efforts to reduce catalyst loading

2.2 Core-shell catalysts

The core-shell structure is an effective method for achieving a balance between the stability and activity of electrocatalysts in PEMWE. It has been demonstrated that the core-shell structure has unique
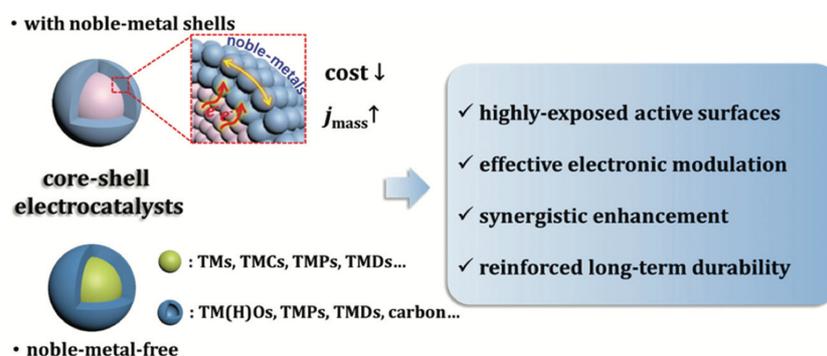
Fig. 6. Schematic overview of core-shell electrocatalyst. Reproduced with permission.[54] Copyright 2020, Royal Society of Chemistry.

physiochemical features resulting from surface strain and atomic localization, which influence charge transfer between the core and shell structures. Strong interactions between the shell and the core result in charge redistributions of shell species, which can further enhance the intrinsic catalytic activity. In addition, the electrochemically stable shell protects the OER-active core, resulting in a synergistic effect that breaks the traditional trade-off between activity and stability.[52,53]

One of the most successful approaches to Ir loading reduction, while mitigating the performance and durability losses of low-loaded anodes, is through catalyst layer modification of morphologies to achieve core-shell catalysts. This type of morphology promotes Ir loading reduction by depositing most Ir atoms on the shell surface to serve as reaction sites for OER, while less expensive materials reside in the catalyst core such as transition metals like Ni, Co, and Fe which are inexpensive and can form nitride phases for better durability. Alloy core-shell catalysts with a noble metal-rich shell have been proven to enhance OER performance by enabling higher electron conductivity and catalyst accessibility given that Ir is deposited on corrosion-stable and highly conductive materials to ensure sufficient durability of core-shell catalysts.[16,40,55] It has

been demonstrated that core-shell conformation can reduce the overpotential (300 mV) and improve stability (96.7% after 1000 cycles).[56]

The synthetic strategies for nanostructures can be loosely classified as top-down or bottom-up. The former reduces big materials (from microns to centimeters) using various etching processes (e.g., electron or ion beam, laser-beam processing and polishing).[57,58] The latter utilizes the molecular's chemical characteristics to induce self-assembly into useful conformations. Chemical synthesis, chemical vapor deposition (CVD), self-assembly, colloidal aggregation, and film deposition and growth are the most prevalent bottom-up techniques. The size, morphology, facets, and textural features of core–shell electrocatalysts can be controlled by modifying the reaction conditions, such as the precursor concentration, temperature, and surfactant.[57] There are three significant classes for the bottom-up synthesis of core–shell electrocatalysts. **(i) Simultaneous fabrication.** The simultaneous method is typically used to produce catalysts from carbon-coated metals or their compounds, in which the reactants are directly combined to produce a precursor. Then, during the pyrolysis process, metal compounds form the core, while carbon-containing components simultaneously transform into a carbon shell and encase the core.[59]
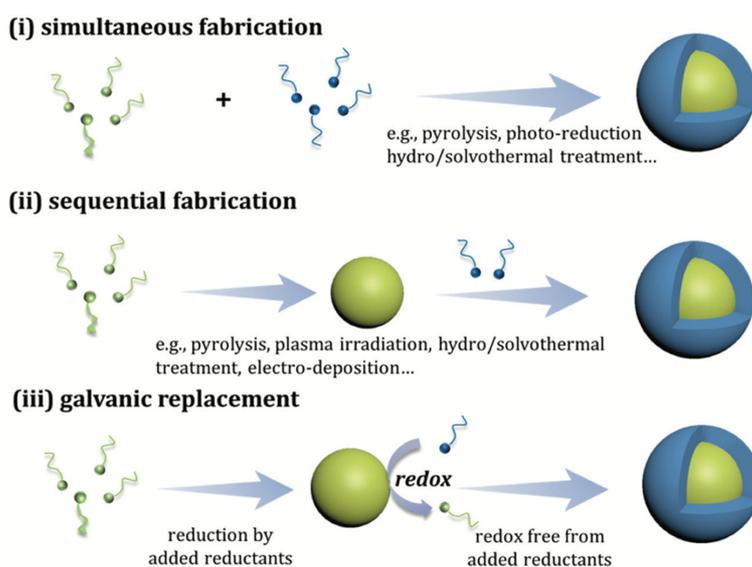

Fig. 7. Synthetic strategies for core-shell electrocatalyst. Reproduced with permission.[54] Copyright 2020, Royal Society of Chemistry.

(ii) Sequential fabrication. It requires additional processes to prepare the core and subsequently the shell. This approach is applicable to all documented core–shell structural nanoparticle composite systems, notwithstanding the unstable nature of some cores. **(iii) Galvanic displacement.** Depending on the potential difference between the two metals, this process involves a redox reaction between the metal core and the required shell ions. It is commonly applied to noble-metal-based core–shell nanostructures and can be carried out in organic or aqueous fluids without additional reducing chemicals.[54]

Galvanic displacement. Although core-shell catalysts show exceptional performance, the process of generating high surface area materials to achieve high specific activity and good durability remains a challenge that can be addressed by different approaches. Galvanic displacement is a common process to achieve core-shell catalysts as this technique is shape-controlled and allows the synthesis of wires, tubes, and particles using a metal "template" with a defined morphology that could be utilized as the less noble metal core to the catalyst system. With


Fig. 8. Schematic of the displacement process. Transmission electron microscopy images of b) Ag nanowire and c) corresponding Pt nanotube following galvanic displacement. Reproduced with permission.[60] Copyright 2014, Royal Society of Chemistry.

this, galvanic displacement occurs spontaneously when the less noble metal template contacts a more noble metal cation, which in this case would be Ir metal. This reaction then combines the aspects of corrosion and electrodeposition to displace less noble metal atoms with Ir metal which therefore yields a catalyst system having deposited Ir shells that takes the shape of the core metal template.[60]

The development of catalysts using galvanic displacement approach is highly motivated in the works of Alia et al. in their attempt to fabricate highly active OER catalysts using Ir-based nanowires. Here, Ir-Ni and Ir-Co nanowires demonstrated a significant specific activity over commercial Ir nanoparticle catalysts by having mass activities 9–10 times higher than Ir nanoparticles in the half-cell tests. The nanowires also further improved durability, exceeding Ir nanoparticles by 4–5 times after post-treatment acid-leaching to remove excess Ni and Co. Overall, this supports possibilities of significant Ir loading reduction in catalysts without compromising performance.[61]

Reductive process. Aside from galvanic displacement, other methods were explored to find more efficient ways to synthesize core-shell nanoparticles. Consequently, facile and scalable chemical reduction method attracted popularity since it allows large scale production at low cost. In this method, metal salt is reduced via a reducing agent in the presence of protective material. Various reducing agents such as sodium citrate, ascorbic acid, hydrazine[62], and ethylene glycol[52,63] which can reduce metallic cations. Several studies[64,65], particularly on Ir based core-shell catalyst have used sodium borohydride ($NaBH_4$), a strong reducing agent, to enable chemical reduction at room temperature. Core-shell nanoparticle formation begins by generating a neutral Ir atom that forms an Ir^{2+} precursor. Consequently, more atoms can be deposited on the surface of the core material which allows to control the shape and size of nanoparticles[66,67]. This technique allowed an Ir mass reduction by a factor of 2 compared to standard IrO_2 electrocatalyst.[64] In fact, the Ir loading of Ir@TiO_2 core-shell catalyst which was synthesized via one-step polyol reduction method[68], was reduced by 60% while increasing the mass activity by 100 times that of commercial IrO_2.
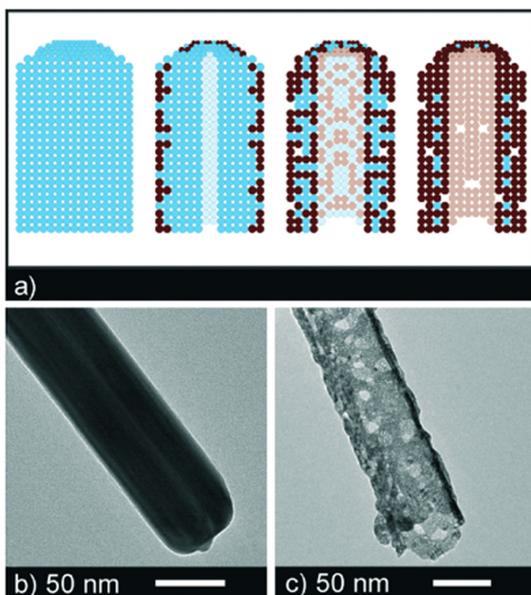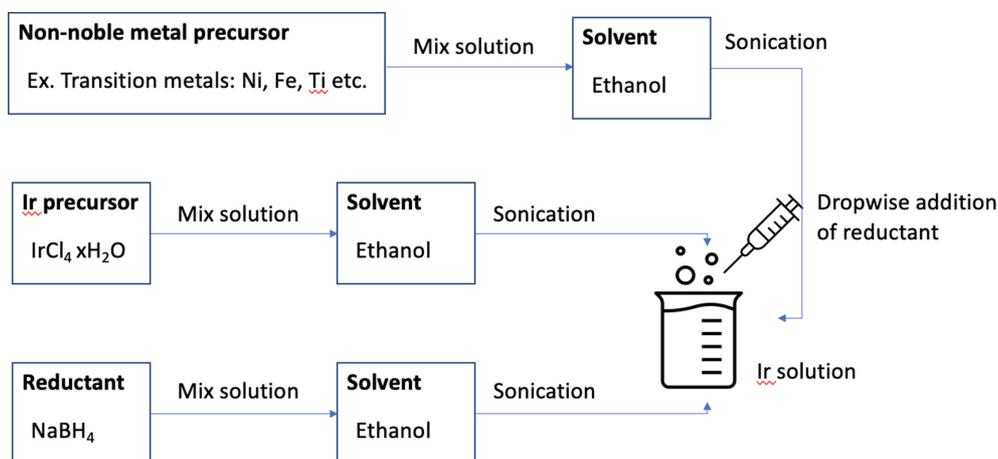
Fig. 9. Scheme of a chemical reduction synthesis for Ir-based catalysts.

Post-synthesis optimizations. Having a core-shell type of morphology in a catalyst makes it adaptable to different types of post-treatment optimizations which allows for better stability and durability. The mention of post-treatment acid leaching was already executed in the earlier studies of Alia et al. that focused more on Pt-based nanowires for ORR at the cathode. Regardless, these post-treatment optimizations, usually after the core-shell synthesis, result in dealloying effects that yield porous noble metal islands and exposed facets. This selective corrosion process formed noble metal islands or skins with certain thickness that contribute in the ensemble effect for high surface stability and durability. Nong et al. also demonstrated IrO$_x$ core-shell nanoparticles in a form of dealloyed metal-oxide hybrid (IrNi@IrO$_x$) by selective surface Ni dealloying and controlled surface oxidation of Ir.[52]

A recent study on IrNi oxide films demonstrates a highly increased catalytic activity (20-fold higher mass activity than IrO$_2$ at 1.53 V RHE) along with a significant Ni dissolution of up to 80% loss of Ni content in the initial OER scans. According to Reier et al., this causes a favorable surface modification that is responsible for the increase in activity.[68] The remaining 12% Ni content appears to be stabilized by the Ir oxide matrix, and while the steady-state Ni content appears to be independent of the initial composition, the morphology is not. In the instance of IrNi oxide nanoparticles, a metal-lic alloy is generated and then electrochemically oxidized, while nickel atoms leach from the particle surfaces. This selective leaching produces particles with a core–shell structure comparable to those of sophisticated ORR electrocatalysts, but with an Ir-rich, oxidized shell and a metallic IrNi core.[69-70] After the oxidation/leaching stage, particles with a diameter range of 5 to 10 nm and an oxide shell of 2 nm are formed. Throughout these processes, the surface Ni/Ir ratio declines significantly, whereas the O/(Ir+Ni) ratio rises. Combining these findings with XPS and EXAFS data, which indicate that Ni species persist on the surface region, has resulted in a surface structure comparable to that of the suggested thin-film catalysts. It is likely that the electrical and strain effects of the underlying metallic core structure can have further influence. During a preliminary stability test in a three-electrode cell, the IrNi core–shell particles demonstrated a 10-fold improvement in performance at 1.48 V RHE and a lower activity loss compared to pure iridium oxide nanoparticles, thereby making them a more viable candidate electrocatalyst for use in a PEM electrolyzer cell. RuNi nanoparticles have also been reported to have similar effects.[71]

A similar study[72] which also conducted Ni leaching during catalyst activation, stated that this treatment causes lattice vacancies which generate uniquely shorter Ir–O metal ligand linkages and an atypically high number of d-band holes in the irid-

ium oxide shell. Density functional theory simulations reveal that this increase in the formal oxidation state of iridium is responsible for the production of holes on oxygen ligands near lattice vacancies. This suggests that the electrophilic nature of these oxygen ligands renders them amenable to the production of nucleophilic acid–base-type O–O bonds at lower kinetic barriers, resulting in significantly improved reactivities.

Iridium-nickel nitride (IrNiN) core-shell nanoparticles formed a hollow structure after it underwent thermal annealing treatment using NH_3 as the nitrogen precursor at ambient temperature.[73] Recent reports indicate that annealing IrNi nanoparticles at temperatures above 450 ℃ in H_2 causes Ir to segregate to the surface of the IrNi solid alloy cores.[22] The downshifting of the d-band center frequency may have two impacts. One is that the surfaces become less reactive for H_2O oxidation and IrOH production, hence making the Ir shell surfaces more metallic and active for hydrogen evolution. The second is to reduce the hydrogen binding energy to a moderate level, which facilitates the recombination of two H_{ads} atoms on the Ir surfaces.

2.2 Corrosion-resistant catalyst support

Nano-scaled catalysts can obtain their full potential when dispersed on an appropriate support material that ideally exhibit high electrical conductivity and high surface area with exceptional corrosion stability under severely corrosive acidic OER conditions.[16] Employing catalyst support to help increase dispersion and reduce the agglomeration of active catalysts is a popular approach to catalyst loading reduction in PEMWE. The interaction between the support surface and the catalyst determines the level of particle detachment or dissolution during operation. This is influenced by the degree of catalyst immobilization on the support. Interactions range from weak electrostatic attraction to stronger connections via surface chemical bonds or the formation of a coating on the support. These can also affect activity by decreasing or increasing the surface electron density of the catalyst. By altering the activity, the catalyst may be subjected to less stress, as a lower potential is sufficient to induce the desired current density. This ultimately contributes to enhanced stability.[76]

Conventionally, carbon is the most popularly used support material as discussed in section 1.6. Alternative materials that can withstand the harsh conditions of OER have been investigated to address the shortcomings of carbon as catalyst support.

Metal oxides. Among several candidates, Sn, In, W, and Ti-based metal oxides are the most frequently turned to support material since they exhibit good corrosion resistance and strong interaction with catalyst nanoparticles.[78-80] Up to date, Ti-based oxides are known to be the only stable support material that can withstand oxidation. In fact, it has been used in chlorine-alkali electrolysis for years as dimensionally stable anode (DSA) material for years.[81] In the case of TiO_2, it has been investigated in acidic OER applications with favorable SMSI improving the catalytic activity[82-84] due to its diverse nano-morphologies as well as high surface area TiO_2 structures.[82,84-86] Within recent advances, titanium oxynitride ($TiON_x$) supports[18,87-89] attracted attention as its initial screenings revealed that its average macroscopic conductivity can reach values between 3 and 8 S cm^{-1} [87] and at the same time shows good interaction with Ir, the state-of-the-art catalyst for OER. $TiON_x$ can be prepared from titanium nitride (TiN) or titanium dioxide (TiO_2) in

Table 3. Summary of synthesis techniques and electrochemical properties of Ir-based core-shell catalysts

Sample	Core / shell	Method / treatment	wt.% Ir	i_m (A/mg)	η_{10} (mV)	ref
Ir@TiO_2	TiO_2 / Ir	polyol reduction	21.8	0.486	220	[75]
Ir-Ni	Ni / Ir	galvanic displacement	9.3	3	-	[61]
Ir-Co	Co / Ir	/ acid leaching	4.2	1	-	[61]
Ir-O_2-2Ti	TiO_2 / Ir	reduction by $NaBH_4$	-	1.38	342	[72]
Ru@ IrO_X	Ru / IrO_X	sequential polyol method	-	0.645	282	[76]
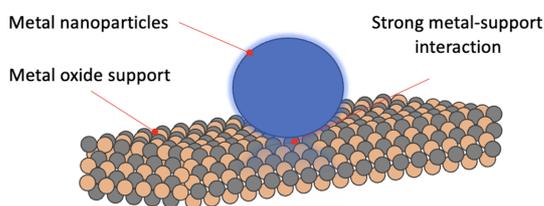
Fig. 10. Schematic illustration of strong metal-support interaction.

various forms using different syntheses methods such as radio frequency (RF) plasma,[90] chemical reduction method, low-pressure chemical vapor deposition (LPCVD),[91] and anodic oxidation.[18] The anodic oxidation synthesis, resulted to a $TiON_x$-Ir support derived from anodically grown TiO_2 nanotubes that exhibit a mass activity that is 5 times better than commercial IrO_2 and 2 times better than $TiON_x$-Ir with different morphologies.[18] Nguyen et al. designed Ir-oxygen of hydroxyl-rich blue TiO_2 (Ir-O_2-2Ti) nanoclusters via chemical reduction method where $NaBH_4$ was utilized as a reductant to covalently bond Ir on blue TiO_2. Remarkably, Ir-O_2-2Ti exhibits a mass activity of 1.38 A/mg$_{Ir}$ at an overpotential of 350 mV which is 27 times greater than commercial IrO_2.[71]

Synthetic diamond. Due to their broader potential window, low background currents, higher chemical inertness, high thermal conductivity, and excellent mechanical stability, BDD electrodes have supplanted glassy carbon and graphite as desirable material for electrochemical applications. The large overpotential for both oxygen and hydrogen evolution is responsible for the wide potential window (the widest recorded to date in aqueous electrolytes) and permits the conversion of molecules with high oxidation and reduction potentials. Diamond's C-sp^3 hybridization, which has a low capacitance and precludes surface oxide development, contributes to its chemical inertness and low background currents. BDD is a material renowned for its low adsorption, resistance to (bio)fouling, great response stability, and high current signal-to-noise ratio, which has made it suitable for a variety of electroanalytical applications for both inorganic and organic chemicals.[92] Typically, boron-doped diamond (BDD) electrodes are deposited on conductive substrates for use in electrochemical oxidation. The BDD exhibits exceptional electrochemical characteristics and chemical resistance for oxygen and hydrogen evolution reactions operating at exceptionally high voltages. Al-Abdallat et al. investigated the catalytic electrochemical water splitting process using a boron-doped diamond (BDD/Nb) electrode. Results suggest that solar energy may be used to drive the efficient catalytic electrochemical water splitting utilizing BDD/Nb electrodes to produce hydrogen gas that can be used directly as a fuel in hydrogen internal combustion engines and proton exchange membrane fuel cells (PEMFCs). It may also be used indirectly to produce methanol via methanol synthesis from CO_2 hydrogenation, with the methanol subsequently being used in direct methanol fuel cells (DMFCs).[93]

Hybrid. A study by Lončar et al. demonstrated a

Table 4. Summary of synthesis techniques and electrochemical properties of Ir-based supported catalysts

Catalyst	Support	Method / treatment	wt.% Ir	i_m (A/mg)	η_{10} (mV)	ref
Ir/ATO	ATO	reduction using ethylene glycol	11	1.1	-	[97]
$IrOOH_x$/ TiO_2	TiO_2	molten salt oxidation route in $NaNO_3$	30	0.62	300	[98]
$TiON_x$-Ir	$TiON_x$	anodic oxidation of Ti foil / deposition of Ir	11	0.520	-	[18]
IrO_2@Ir/TiN	TiN	reduction using ethylene glycol	60	0.480	265	[99]
IrO_2-TiO_2	TiO_2	adams fusion method	40 mol$_M$	-	255	[59]
IrO_x/$SrIrO_3$	$SrIrO_3$	reduction using $NaBH_4$	30	-	270	[85]
np-Ir/ NiFeO	NiFeO	selective etching	0.1	39.3	197	[100]
NPG@Pt/Ir	NPG	galvanic displacement	-	-	230	[101]
IrO_2@NiO	NiO/Ni foam	-	0.62		278	[102]

unique core-shell-supported hybrid catalyst using a novel synthesis method. Herein, Ir nanoparticles are efficiently attached on a conductive substrate titanium oxynitride (TiON$_x$) spread over carbon-based KetjenBlack and covered by a thin copper layer (Ir/ CuTiON$_x$/C), which is removed during the preconditioning stage. This technique initially combines both the core-shell strategy and at the same time employs a support material for an enhanced SMSI effect. Utilization of these advanced methods indicated that the sacrificial Cu layer positively affects both Ir OER mass activity and its endurance. The increased surface area of smaller Ir nanoparticles, which are better maintained by a strong metal-support interaction (SMSI) effect, was attributed to the enhanced activity of the Cu analog.[100]

3. Conclusion

Due to the intermittency of renewable energy sources, a need to store and transport energy will increase. Hydrogen production through water electrolysis, combined with renewable energy sources, will provide an excellent way to supplement the intermittency of renewable energy sources. While alkaline water electrolysis is currently the most mature technology, it has drawbacks of low current density, large footprint, gas crossover, etc. The PEM water electrolysis has potential to replace the alkaline electrolysis. However, expensive catalyst material used in the PEM electrolysis has been the bottleneck of widespread use. In this review, we have reviewed recent efforts to reduce catalyst loading in PEM water electrolysis. In core-shell nanostructures, the precious metal catalyst forms a shell while heteroatoms form a core. In this way, the catalyst loading can be significantly reduced while maintaining the catalytic activity. In another approach, a corrosion-resistant support is utilized, which provides a stable platform to impregnate precious metal catalyst.

Acknowledgment

References

[1] N. Du, C. Roy, R. Peach, M. Turnbull, S. Thiele, and C. Bock, Anion-Exchange Membrane Water Electrolyzers, *Chemical Reviews*, **122(13)**, 11830 (2022).

[2] M. Carmo, D. L. Fritz, J. Mergel, and D. Stolten, A comprehensive review on PEM water electrolysis, *Int. J. Hydrogen Energy*, **38(12)**, 4901 (2013).

[3] W. T. Grubb, Batteries with Solid Ion Exchange Electrolytes I. Secondary Cells Employing Metal Electrodes, *J. Electrochem. Soc.*, **165(4)**, 275 (1959)

[4] W. T. Grubb, IONIC MIGRATION IN ION-EXCHANGE MEMBRANES, *J. Phys. Chem.*, **63(1)**, 59 (1959).

[5] P. Medina and M. Santarelli, Analysis of water transport in a high pressure PEM electrolyzer, *Int. J. Hydrogen Energy*, **35(11)**, 5173 (2010).

[6] K. E. Ayers *et al.*, Research Advances towards Low Cost, High Efficiency PEM Electrolysis, *ECS Trans*, **33(1)**, 3 (2010).

[7] R. H. Mitchell and R. R. Keays, Abundance and distribution of gold, palladium and iridium in some spinel and garnet Iberzolites: implications for the nature and origin of precious metal-rich intergranular components in the upper mantle, *Geochemica et Cosmochimica Acta*, **45(12)**, 2425 (1981).

[8] L. B. Hunt, A History of Iridium Overcoming the Difficulties of Melting and Fabrication, *Platinum Metals Rev.*, **31(1)**, 32 (1987).

[9] S. J. Parry, Abundance and Distribution of Palladium, Platinum, Iridium and Gold in Some Oxide Minerals, *Chemical Geology*, **43**, 115 (1984).

[10] B. Huang and Y. Zhao, Iridium-based electrocatalysts toward sustainable energy conversion, *EcoMat*, **4(2)**, 2022.

[11] J. Chen, S. Jayabal, D. Geng, and X. Hu, Monolayer Iridium Nanoparticles Coated TiO$_2$ Core-Shell Architecture as Efficient Oxygen Evolution Reaction Electrocatalyst, *Chemistry Select*, **6(34)**, 9134 (2021).

[12] M. H. Miles and M. A. Thomason, Periodic Variations of Overvoltages for Water Electrolysis in Acid Solutions from Cyclic Voltammetric Studies, *ECS*, **123(10)**, 1459 (1976).

[13] D. Galizzioli, F. Tantardini, and S. Trasatti, Ruthenium dioxide: A new electrode material. I. Behaviour in acid solutions of inert electrolytes, *J. Applied Electrochemistry*, **4**, 57 (1974).

[14] M. Tahir *et al.*, Electrocatalytic oxygen evolution reaction for energy conversion and storage: A comprehensive review, *Nano Energy*, **37**, 136 (2017).

[15] S. Cherevko, A. R. Zeradjanin, A. A. Topalov, N. Kulyk, I. Katsounaros, and K. J. J. Mayrhofer, Dissolution of noble metals during oxygen evolution in acidic media, *Chem. Cat. Chem.*, **6(8)**, 2219 (2014).

[16] T. Reier, H. N. Nong, D. Teschner, R. Schlögl, and P. Strasser, Electrocatalytic Oxygen Evolution Reaction in

Acidic Environments – Reaction Mechanisms and Catalysts, *Adv. Energy Mater*, **7(1)**, 1601275 (2017).

[17] C. He, *Corrosion-Resistant Non-Carbon Electrocatalyst Supports for Corrosion-Resistant Non-Carbon Electrocatalyst Supports for Proton Exchange Membrane Fuel Cells Proton Exchange Membrane Fuel Cells*, PhD Dissertation, Washington University in St. Louis, Missouri, USA (2019).

[18] L. Moriau, M. Bele, Z. Marinko, F. Ruiz-Zepeda, G. K. Podborsek, M. Sala, A. K. Surca, J. Kovac, I. Arcon, P. Jovanovic, N. Hodnik, and L. Suhadolnik, Effect of the Morphology of the High-Surface-Area Support on the Performance of the Oxygen-Evolution Reaction for Iridium Nanoparticles, *ACS Catal*, **11(2)**, 670 (2021).

[19] L. Du, Y. Shao, J. Sun, G. Yin, J. Liu, and Y. Wang, Advanced catalyst supports for PEM fuel cell cathodes, *Nano Energy*, **29**, 314 (2016).

[20] H. Chhina, S. Campbell, and O. Kesler, An oxidation-resistant indium tin oxide catalyst support for proton exchange membrane fuel cells, *J. Power Sources*, **161(2)**, 893 (2006).

[21] C. V. Subban, Q. Zhou, A. Hu, T. E. Moylan, F. T. Wagner, and F. J. Disalvo, Sol-gel synthesis, electrochemical characterization, and stability testing of $Ti_{0.7}W_{0.3}O_2$ nanoparticles for catalyst support applications in proton-exchange membrane fuel cells, *J. Am. Chem. Soc.*, **132(49)**, 17531 (2010).

[22] S. Y. Huang, P. Ganesan, and B. N. Popov, Titania supported platinum catalyst with high electrocatalytic activity and stability for polymer electrolyte membrane fuel cell, *Appl. Catal B*, **102(1–2)**, 171 (2011).

[23] S. Y. Huang, P. Ganesan, S. Park, and B. N. Popov, Development of a titanium dioxide-supported platinum catalyst with ultrahigh stability for polymer electrolyte membrane fuel cell applications, *J. Am. Chem. Soc.*, **131(39)**, 13898 (2009).

[24] V. T. T. Ho, C. J. Pan, J. Rick, W. N. Su, and B. J. Hwang, Nanostructured $Ti_{0.7}Mo_{0.3}O_2$ support enhances electron transfer to Pt: High-performance catalyst for oxygen reduction reaction, *J. Am. Chem. Soc.*, **133(30)**, 11716 (2011).

[25] P. Goswami and J. N. Ganguli, Tuning the band gap of mesoporous Zr-doped TiO2 for effective degradation of pesticide quinalphos, *Dalton Transactions*, **42(40)**, 14480 (2013).

[26] L. Li, W. Yang, Y. Ding, and X. Zhu, First principle study of the electronic structure of hafnium-doped anatase TiO2, *J. Semiconductors*, **33(1)**, 012002-1 (2012).

[27] J. H. Kim, G. Kwon, H. Lim, C. Zhu, H. You, and Y. T. Kim, Effects of transition metal doping in Pt/M-TiO2 (M = V, Cr, and Nb) on oxygen reduction reaction activity, *J. Power Sources*, **320**, 188 (2016).

[28] C. Beauger, L. Testut, S. Berthon-Fabry, F. Georgi, and L. Guetaz, Doped TiO2 aerogels as alternative catalyst supports for proton exchange membrane fuel cells: A comparative study of Nb, v and Ta dopants, *Micropo-rous and Mesoporous Materials*, **232**, 109 (2016).

[29] S. Sun, G. Zhang, X. Sun, M. Cai, and M. Ruthkosky, Highly stable and active Pt/Nb-TiO2 carbon-free electrocatalyst for proton exchange membrane fuel cells, *J. Nanotechnol*, (2012).

[30] L. Chevallier, A. Bauer, S. Cavaliere, R. Hui, J. Rozière, and D. J. Jones, Mesoporous nanostructured Nb-doped titanium dioxide microsphere catalyst supports for PEM fuel cell electrodes, *ACS Appl. Mater Interfaces*, **4(3)**, 1752 (2012).

[31] A. Bauer, L. Chevallier, R. Hui, S. Cavaliere, J. Zhang, D. Jones, and J. Roziere, Synthesis and characterization of Nb-TiO2 mesoporous microsphere and nanofiber supported Pt catalysts for high temperature PEM fuel cells, *Electrochim. Acta*, **77**, 1 (2012).

[32] H. A. Huy, B. Aradi, T. Frauenheim, and P. Deák, Comparison of Nb- and Ta-doping of anatase TiO2 for transparent conductor applications, *J. Applied Physics*, **112(1)**, 016103 (2012).

[33] S. L. Gojković, B. M. Babić, V. R. Radmilović, and N. V. Krstajić, Nb-doped TiO2 as a support of Pt and Pt-Ru anode catalyst for PEMFCs, *J. Electroanalytical Chemistry*, **639(1–2)**, 161 (2010).

[34] T. B. Do, M. Cai, M. S. Ruthkosky, and T. E. Moylan, Niobium-doped titanium oxide for fuel cell application, *Electrochimica Acta*, **55(27)**, 8013 (2010).

[35] K. W. Park and K. S. Seol, Nb-TiO2 supported Pt cathode catalyst for polymer electrolyte membrane fuel cells, *Electrochem. commun*, **9(9)**, 2256 (2007).

[36] A. Kumar and V. Ramani, $Ta_{0.3}Ti_{0.7}O_2$ Electrocatalyst Supports Exhibit Exceptional Electrochemical Stability, *J. Electrochem Soc.*, **160(11)**, F1207 (2013).

[37] C. P. Lo, G. Wang, A. Kumar, and V. Ramani, TiO2-RuO2 electrocatalyst supports exhibit exceptional electrochemical stability, *Appl. Catal B*, **140–141**, 133 (2013).

[38] X. Li, Z. Guo, and T. He, The doping mechanism of Cr into TiO2 and its influence on the photocatalytic performance, *Physical Chemistry Chemical Physics*, **15(46)**, 20037 (2013).

[39] R. Alipour Moghadam Esfahani, S. K. Vankova, A. H. A. Monteverde Videla, and S. Specchia, Innovative carbon-free low content Pt catalyst supported on Mo-doped titanium suboxide (Ti3O5-Mo) for stable and durable oxygen reduction reaction, *Appl. Catal B*, **201**, 419 (2017).

[40] F. Hegge F. Lombeck, E. C. Ortiz, L. Bohn, M. v. Holst, M. Korschel, J. Hubner, M. Breitwieser, P. Strasser, and S. Vierrath, Efficient and Stable Low Iridium Loaded Anodes for PEM Water Electrolysis Made Possible by Nanofiber Interlayers, *ACS Appl Energy Mater*, **3(9)**, 8276 (2020).

[41] Y. Liu and W. E. Mustain, Structural and electrochemical studies of Pt clusters supported on high-surface-area tungsten carbide for oxygen reduction, *ACS Catal*, **1(3)**, 212 (2011).

[42] Y. Liu and W. E. Mustain, Evaluation of tungsten carbide as the electrocatalyst support for platinum hydrogen evolution/oxidation catalysts, *Int. J. Hydrogen. Energy*, **37(11)**, 8929 (2012).

[43] D. v. Esposito and J. G. Chen, Monolayer platinum supported on tungsten carbides as low-cost electrocatalysts: Opportunities and limitations, *Energy Environ. Sci.*, **4(10)**, 3900 (2011).

[44] N. Cheng, M. N. Banis, J. Liu, A. Riese, S. Mu, R Li, T. K. Sham, and X. Sun, Atomic scale enhancement of metal-support interactions between Pt and ZrC for highly stable electrocatalysts, *Energy Environ. Sci.*, **8(5)**, 1450 (2015).

[45] H. J. Liu, F. Wang, Y. Zhao, and H. Fong, Mechanically resilient electrospun TiC nanofibrous mats surface-decorated with Pt nanoparticles for oxygen reduction reaction with enhanced electrocatalytic activities, *Nanoscale*, **5(9)**, 3643 (2013).

[46] S. N. Stamatin, J. Speder, R. Dhiman, M. Arenz, and E. M. Skou, Electrochemical stability and postmortem studies of Pt/SiC catalysts for polymer electrolyte membrane fuel cells, *ACS Appl Mater Interfaces*, **7(11)**, 6153 (2015).

[47] Y. Nabil, S. Cavaliere, I. A. Harkness, G. A. Hards, J. S. Sharman, D. J. Jones, and J. Roziere, Corrosion Resistant Electrospun Niobium Carbide Nanotube Supports for PEMFC Cathodes, *ECS Trans*, **69(17)**, 1221 (2015).

[48] S. Jayabal, G. Saranya, D. Geng, L. Y. Lin, and X. Meng, Insight into the correlation of Pt-support interactions with electrocatalytic activity and durability in fuel cells, *J. Mat. Chem. A*, **8(19)**, 9420 (2020).

[49] H. Nan, D. Dang, and X. L. Tian, Structural engineering of robust titanium nitride as effective platinum support for the oxygen reduction reaction, *J. Mater Chem. A Mater*, **6(14)**, 6065 (2018).

[50] Y. Xiao, G. Zhan, Z. Fu, Z. Pan, C. Xiao, S. Wu, C. Chen, G. Hu, and Z. Wei, Titanium cobalt nitride supported platinum catalyst with high activity and stability for oxygen reduction reaction, *J, Power Sources*, **284**, 296 (2015).

[51] S. Yang, J. Kim, Y. J. Tak, A. Soon, and H. Lee, Single-Atom Catalyst of Platinum Supported on Titanium Nitride for Selective Electrochemical Reactions, *Angewandte Chemie*, **128(6)**, 2098 (2016).

[52] H. N. Nong, L. Gan, E. Willinger, D. Teschner, and P. Strasser, IrOx core-shell nanocatalysts for cost- and energy-efficient electrochemical water splitting, *Chem. Sci.*, **5(8)**, 2955 (2014).

[53] K. W. Ahmed, M. J. Jang, M. G. Park, Z. Chen, and M. Fowler, Effect of Components and Operating Conditions on the Performance of PEM Electrolyzers: A Review, *Electrochem.*, **3(4)**, 581 (2022).

[54] X. Yin, L. Yang, and Q. Gao, Core-shell nanostructured electrocatalysts for water splitting, *Nanoscale*, **12(30)**, 15944 (2020).

[55] H. S. Oh, H. N. Nong, T. Reier, M. Gliech, and P. Strasser, Oxide-supported Ir nanodendrites with high activity and durability for the oxygen evolution reaction in acid PEM water electrolyzers, *Chem. Sci.*, **6(6)**, 3321 (2015).

[56] T. Audichon, T. W. Napporn, C. Canaff, C. Morais, C. Comminges, and K. B. Kokoh, IrO$_2$ Coated on RuO2 as Efficient and Stable Electroactive Nanocatalysts for Electrochemical Water Splitting, *J. Phy. Chem. C*, **120(5)**, 2562 (2016).

[57] S. Wei, Q. Wang, J. Zhu, L. Sun, H. Lin, and Z. Guo, Multifunctional composite core-shell nanoparticles, *Nanoscale*, **3(11)**, 4474 (2011).

[58] R. Ghosh Chaudhuri and S. Paria, Core/shell nanoparticles: Classes, properties, synthesis mechanisms, characterization, and applications, *Chemical Reviews*, **112(4)**, 2373 (2012).

[59] H. Lin, Z. Shi, S. He, X. Yu, S. Wang, Q. Gao, and Y. Tang, Heteronanowires of MoC-Mo$_2$C as efficient electrocatalysts for hydrogen evolution reaction," *Chem. Sci.*, **7(5)**, 3399 (2016).

[60] S. M. Alia, Y. S. Yan, and B. S. Pivovar, Galvanic displacement as a route to highly active and durable extended surface electrocatalysts, *Catal Sci. Technol.*, **4(10)**, 3589 (2014).

[61] S. M. Alia, S. Shulda, C. Ngo, S. Pylypenko, and B. S. Pivovar, Iridium-Based Nanowires as Highly Active, Oxygen Evolution Reaction Electrocatalysts, *ACS Catal*, **8(3)**, 2111 (2013).

[62] S. M. Alia, B. S. Pivovar, and Y. Yan, Platinum-coated copper nanowires with high activity for hydrogen oxidation reaction in base, *J. Am. Chem. Soc.*, **135(36)**, 13473 (2013).

[63] S. M. Alia, K. O. Jensen, B. S. Pivovar, and Y. Yan, Platinum-coated palladium nanotubes as oxygen reduction reaction electrocatalysts, *ACS Catalysis*, **2(5)**, 858 (2012).

[64] B. M. Tackett, W. Sheng, S. Katte, S. Yao, B. Yan, K. A. Kuttiyiel, Q. Wu, and J. G. Chen, Reducing Iridium Loading in Oxygen Evolution Reaction Electrocatalysts Using Core-Shell Particles with Nitride Cores, *ACS Catalysis*, **8(3)**, 2615 (2018).

[65] P. Lettenmeier, J. Majchel, L. Wang, V. A. Saveleva, S. Zafeiratos, e. R. Savinova, J. J. Gallet, F. Bournel, A. S. Gago, and K. A. Friedrich, Highly active nano-sized iridium catalysts: Synthesis and operando spectroscopy in a proton exchange membrane electrolyzer, *Chem. Sci.*, **9(14)**, 3570 (2018).

[66] C. A. dos Santos, M. M. Seckler, A. P. Ingle, I. Gupta, S. Galdiero, M. Galdiero, A. Gade, and M. Rai, Silver nanoparticles: Therapeutical uses, toxicity, and safety issues, *J. Pharm. Sci.*, **103(7)**, 1931 (2014).

[67] V. Raji, M. Chakraborty, and P. A. Parikh, Synthesis of starch-stabilized silver nanoparticles and their antimicrobial activity, *Particulate Sci. Tech.*, **30(6)**, 565 (2012).

[68] T. Reier, Z. Pawolek, S. Cherevko, M. Bruns, T. Jones, D. Teschner, S. Selve, A. Bergmann, H. N. Nong, R.

Schlogl, K. J. J. Mayrhofer, and P. Strasser, Molecular insight in structure and activity of highly efficient, low-Ir Ir-Ni oxide catalysts for electrochemical water splitting (OER), *J. Am. Chem. Soc.*, **137(40)**, 13031 (2015).

[69] N. B. Halck, V. Petrykin, P. Krtil, and J. Rossmeisl, Beyond the volcano limitations in electrocatalysis-oxygen evolution reaction, *Physical Chemistry Chemical Physics*, **16(27)**, 13682 (2014).

[70] R. Yang, P. Strasser, and M. F. Toney, Dealloying of Cu_3Pt (111) studied by surface X-ray scattering," *J. Physical Chemistry C*, **115(18)**, 9074 (2011).

[71] C. T. K. Nguyen, N. Q. Tran, T. A. Le, and H. Lee, Covalently bonded Ir (IV) on conducted blue TiO_2 for efficient electrocatalytic oxygen evolution reaction in acid media, *Catalysts*, **11(10)**, 1176 (2010).

[72] H. N. Nong, T. Reier, H. S. Oh, M. Gliech, P. Paciok, T. H T. Vu, D. Teschner, M. Heggen, V. Petkov, R. Schlogl, T. Jones, and P. Strasser, A unique oxygen ligand environment facilitates water oxidation in hole-doped IrNiOx core–shell electrocatalysts, *Nat Catal*, **1(11)**, 841 (2018).

[73] K. A. Kuttiyiel, K. Sasaki, W.-F. Chen, D. Su, and R. R. Adzic, Core-Shell, Hollow-Structured Iridium-Nickel Nitride Nanoparticles for the Hydrogen Evolution Reaction, *J. Mater. Chem. A*, **2**, 591 (2014).

[74] N. T. Suen, S. F. Hung, Q. Quan, N. Zhang, Y. J. Xu, and H. M. Chen, Electrocatalysis for the oxygen evolution reaction: Recent development and future perspectives, *Chem. Soc. Rev.*, **46(2)**, 337 (2017).

[75] J. Shan, c. Guo, Y. Zhu, M. Jaroniec, Y. Zheng, S. Z. Qiao, Charge-Redistribution-Enhanced Nanocrystalline Ru@IrOx Electrocatalysts for Oxygen Evolution in Acidic Media, *Chem*, **5(2)**, 445 (2019).

[76] L. Yu, Y. Liu, F. Yang, J. Evans, J. A. Rodriguez, and P. Liu, CO Oxidation on Gold-Supported Iron Oxides: New Insights into Strong Oxide-Metal Interactions, *J. Physical Chemistry C*, **119(29)**, 16614 (2015).

[77] P. Zhang, S.-Y. Huang, and B. N. Popov, Mesoporous Tin Oxide as an Oxidation-Resistant Catalyst Support for Proton Exchange Membrane Fuel Cells, *J. Electrochem. Soc.*, **157(8)**, B1163 (2010).

[78] T. Ioroi, H. Senoh, S. Yamazaki, Z. Siroma, N. Fujiwara, and K. Yasuda, Stability of Corrosion-Resistant Magnéli-Phase Ti[sub 4]O[sub 7]-Supported PEMFC Catalysts at High Potentials, *J. Electrochem. Soc.*, **155(4)**, B321 (2008).

[79] Y. Liu and W. E. Mustain, High stability, high activity Pt/ITO oxygen reduction electrocatalysts, *J. Am. Chem. Soc.*, **135(2)**, 530 (2013).

[80] O. Lori and L. Elbaz, Advances in ceramic supports for polymer electrolyte fuel cells, *Catalysts*, **5(3)**, 1445 (2015).

[81] S. Trasatti, Electrocatalysis: understanding the success of DSA®, *Electrochimica Acta*, **45(15-16)**, 2377 (2000).

[82] E. Oakton, IrO_2-TiO_2: A High-Surface-Area, Active, and Stable Electrocatalyst for the Oxygen Evolution Reac-

tion, *ACS Catal*, **7(4)**, 2346 (2017).

[83] T. Reier, D. Teschner, T. Lunkenbein, A. Bergmann, S. Selve, R. Schlogl, and P. Strasser, Electrocatalytic Oxygen Evolution on Iridium Oxide: Uncovering Catalyst-Substrate Interactions and Active Iridium Oxide Species, *J. Electrochem Soc.*, **161(9)**, F876(2014).

[84] T. Reier, I. Weidinger, P. Hildebrandt, R. Kraehnert, and P. Strasser, Electrocatalytic Oxygen Evolution Reaction on Iridium Oxide Model Film Catalysts: Influence of Oxide Type and Catalyst Substrate Interactions, *ECS Trans*, **58(2)**, 39 (2013).

[85] P. Mazúr, J. Polonský, M. Paidar, and K. Bouzek, Non-conductive TiO_2 as the anode catalyst support for PEM water electrolysis, *Int. J. Hydrogen. Energy*, **37(17)**, 12081 (2012).

[86] H. Yoo, K. Oh, Y. R. Lee, K. H. Row, G. Lee, and J. Choi, Simultaneous co-doping of RuO_2 and IrO_2 into anodic TiO_2 nanotubes: A binary catalyst for electrochemical water splitting, *Int. J. Hydrogen. Energy*, **42(10)**, 6657 (2017).

[87] M. Bele, K. Stojanovski, P. Javanovic, L. Moriau, G. K. Podborsek, P. Moskon, P. Umek, M. Sluban, G. Drazic, N. Hodnik, and M. Gaberscek, Towards Stable and Conductive Titanium Oxynitride High Surface Area Support for Iridium Nanoparticles as Oxygen Evolution Reaction Electrocatalyst, *Chem. Cat. Chem.*, **11(20)**, 5038 (2019).

[88] M. Bele, P. Jovanovic, Z. Marinko, S. Drev, V. S. Selih, J. Kovac, M. Gaberscek, G. K. Podbersek, G. Drazic, N. Hodnik, A. Kokalj, and L. Suhadiljhik, Increasing the Oxygen-Evolution Reaction Performance of Nanotubular Titanium Oxynitride-Supported Ir Nanoparticles by a Strong Metal–Support Interaction, *ACS Catal*, **10(22)**, 13688 (2020).

[89] L. Moriau, G. K. Podborsek, A. K. Surca, S. S. Parpari, M. Sala, U. Petek, M. Bele, P. Jovanovic, B. Genorio, and Nejc Hodnik, Enhancing Iridium Nanoparticles' Oxygen Evolution Reaction Activity and Stability by Adjusting the Coverage of Titanium Oxynitride Flakes on Reduced Graphene Oxide Nanoribbons' Support, *Adv. Mater Interfaces*, **8(17)**, 2100900 (2021).

[90] F. M. El-Hossary, N. Z. Negm, A. M. Abd El-Rahman, M. Raaif, and A. A. Abd Elmula, Properties of Titanium Oxynitride Prepared by RF Plasma, *Adv. Chem. Eng. Sci.*, **5(1)**, 1 (2015).

[91] X. Song, D. Gopireddy, and C. G. Takoudis, Characterization of titanium oxynitride films deposited by low pressure chemical vapor deposition using amide Ti precursor, *Thin Solid Films*, **516(18)**, 6330 (2008).

[92] J. Roeser, N. F. A. Alting, H. P. Permentier, A. P. Bruins, and R. Bischoff, Boron-doped diamond electrodes for the electrochemical oxidation and cleavage of peptides, *Anal. Chem.*, **85(14)**, 6626 (2013).

[93] Y. Al-Abdallat, I. Jumah, R. Jumah, H. Ghanem, and A. Telfah, Catalytic electrochemical water splitting using boron doped diamond (BDD) electrodes as a promising energy resource and storage solution, *Energies (Basel)*,

13(20), 5265 (2020).

[94] A. Hartig-Weiss, M. Miller, H. Beyer, A. Schmitt, A. Siebel, A. T. S. Freiberg, H. A. Gasteiger, and H. A. El-Sayed, Iridium Oxide Catalyst Supported on Antimony-Doped Tin Oxide for High Oxygen Evolution Reaction Activity in Acidic Media, *ACS Appl Nano Mater*, **3(3)**, 2185 (2020).

[95] D. Böhm, M. Beetz, C. Gebauer, M. Bernt, J. Schroter, M. Kornherr, F. Zoller, T. Bein, and D. Fattakhova-Rohlfing, Highly conductive titania supported iridium oxide nanoparticles with low overall iridium density as OER catalyst for large-scale PEM electrolysis, *Appl Mater Today*, **24**, 101134 (2021).

[96] G. Li, K. L. L. Yang, J. Chang, R. Ma, Z. Wu, J. Ge, C. Liu, and W. Xing, Boosted Performance of Ir Species by Employing TiN as the Support toward Oxygen Evolution Reaction, *ACS Appl Mater Interfaces*, **10(44)**, 38117 (2018).

[97] K. Jiang, M. Luo, M. Peng, Y. Yu, Y. R. Lu, T. S. Chan, P. Liu, F. M. F. d. Groot, and Y. Tan, Dynamic active-site generation of atomic iridium stabilized on nanoporous metal phosphides for water oxidation, *Nat Commun*, **11(1)**, 2701 (2020).

[98] Y. Wang and J. Kim, Oxygen Evolution Reaction on Nanoporous Gold Modified with Ir and Pt: Synergistic Electrocatalysis between Structure and Composition, *Electroanalysis*, **31(6)**, 1026 (2019).

[99] J. Liu, Z. Wang, K. Su, D. Xv, D. Zhao, J. Li, H. Tong, D. Qian, C. Yang, and Z. Lu, Self-Supported Hierarchical IrO2@NiO Nanoflake Arrays as an Efficient and Durable Catalyst for Electrochemical Oxygen Evolution, *ACS Appl Mater Interfaces*, **11(29)**, 25854 (2019).

[100] A. Lončar, D. Escalera-Lopez, F. Ruiz-Zepeda, A. Hrnjic, M. Sala, P. Jovanovic, M. Bele, S. Cherevko, and N. Hodnik, Sacrificial Cu Layer Mediated the Formation of an Active and Stable Supported Iridium Oxygen Evolution Reaction Electrocatalyst, *ACS Catal*, **11(20)**, 12510 (2021).